

# Characterization of Swirling Methane Jet Flames by LDV and Line Raman/LIPF-OH Techniques

T. S. Cheng<sup>1</sup>, Y.-C. Chao<sup>2</sup>, D.-C. Wu<sup>2</sup>, and T. Yuan<sup>2</sup>

<sup>1</sup>Department of Mechanical Engineering  
Chung Hua University  
Hsinchu, Taiwan, 300, ROC  
Phone: 886-3-5374281 ext. 8337  
Fax: 886-3-5373771  
E-mail: tscheng@chu.edu.tw

<sup>2</sup>Institute of Aeronautics and Astronautics  
National Cheng Kung University  
Tainan, Taiwan, 701, ROC

The increasing stringent regulations have direct impact on the various types of current hydrocarbon combustion devices and drive research efforts toward more effective reduction of pollutant emissions from combustion and toward more intrinsic reaction details. Swirling flows are widely employed in industrial and gas turbine burners for increasing fuel-air mixing, intensifying and stabilizing combustion, shortening the flame length, and reducing pollution emissions. There is a large amount of studies on swirling flows and flames in the literature (e.g., Chigier et al., 1970; Claypole and Syred, 1981); however, most of the attention is paid to the characterize the velocity and turbulence fields and quite often intrusive measurement techniques using probes are applied. In order to look further into the formation of pollutant associated with the mixing and combustion processes and to provide quantitative data for combustion modeling, detailed local fluid dynamic, thermodynamic, and chemical properties, such as velocity, mixture fraction, temperature, and species concentration, must be determined.

Laser-based diagnostic methods provide nonintrusive measurement to investigate the combustion flowfields (Eckbreth, 1988). Laser-Doppler Velocimetry (LDV) is a common tool used to determine the velocity of the combustion flowfields. Spontaneous vibrational Raman scattering can provide quantitative simultaneous measurements of temperature and multi-species concentration with a single laser pulse (Drake et al., 1986). UV Raman scattering technique has been successfully applied to measure temperature and multi-species concentration (O<sub>2</sub>, N<sub>2</sub>, H<sub>2</sub>O, and H<sub>2</sub>) in subsonic (Cheng et al., 1992; Nandula et al., 1994; Brockhinke et al., 1995 and Chen and Mansour, 1996) and supersonic (Cheng et al., 1994) hydrogen-air flames. However, only a few UV Raman scattering measurements have been made in methane-air flames (Hassel, 1993; Mansour and Chen, 1996 and Chen et al., 1996). In methane-air flames the number of major species is increased to include CO<sub>2</sub>, O<sub>2</sub>, CO, N<sub>2</sub>, CH<sub>4</sub>, H<sub>2</sub>O, and H<sub>2</sub>. The increased number of species and the small wavelength difference of the Raman lines, especially the Stokes signals of CO<sub>2</sub> and O<sub>2</sub>, and CO and N<sub>2</sub>, cause difficulties in separation of the species. To obtain the quantitative single-shot measurement in turbulent methane flames, the detailed analysis of laminar flame spectra and spectral background for various equivalence ratios has been made (Cheng et al., 1998a). In this paper, a swirling flame ( $S = 1.0$ ,  $MR = 1.5$ ) with axial fuel injection is studied. LDV is used to determine the fluid dynamic properties of the flowfields. Line Raman scattering and laser-induced predissociative fluorescence (LIPF) techniques are combined to simultaneously measure temperature, mixture fraction, major species concentrations, and OH radical concentration in the flames.

The experimental setup of the LDV system has been described elsewhere (Cheng et al., 1998b). The UV line Raman system is shown in Fig. 1. Details of the Raman system have been reported previously (Cheng et al., 1998a), and only a brief description is included in this paper. The Lambda-Physik LPX-250T narrowband KrF excimer laser produces light that is tunable from 247.9 to 248.9 nm with a bandwidth of  $\sim 0.003$  nm and a pulse energy of  $\sim 400$  mJ. The laser is tuned to 248.56 nm for major species and OH concentration measurements while keeps O<sub>2</sub> fluorescence signals minimum. Light scattered by the 2000 mm focusing lens is measured by a photomultiplier (PMT) to provide a relative measure of laser pulse energy. The laser beam is focused into either the flat-flame "Hencken" burner for calibration or the swirl burner for measurements. Fluorescence and Stokes Raman scattering signals are collected by two separate Cassegrainian mirrors and focused into two spectrometers each coupled with an ICCD camera; the SPEX 500M spectrometer for measuring CO<sub>2</sub>, O<sub>2</sub>, CO, N<sub>2</sub>, and CH<sub>4</sub> and the Spectra Pro-275 spectrometer for detecting, H<sub>2</sub>O, H<sub>2</sub>, and OH. The Raman and fluorescence signals from the camera are digitized with a 14-bit A/D card connected to a personal computer for data processing. The camera image of the laser line is 3.31 mm in length, a value determined by the effective width of the CCD chip (7.8 mm)

and the magnification of the collection optics (2.36). In post processing of data, the line image is divided into 8 segments, each with a spatial resolution of 0.41 mm. The Raman/LIPF-OH imaging system is calibrated for all the 8 radial segments over the flat-flame burner at various stoichiometries. The well-calibrated Raman/LIPF-OH system is then used for analyzing the current swirling flames. The swirl burner is schematically shown in Fig. 2. The swirling component is generated by the swirler with six guide vanes at the angle of 45° or 55° which is placed coaxially with the central fuel tube, corresponding to the swirl number of 0.7 and 1.0, respectively. The diameter of the swirler is 30 mm. Methane can be supplied either from an axial injector with  $D = 5$  mm inner diameter or from an annular injector with four 2.5 mm holes inclined by 45° to investigate the effect of fuel injection. The swirl burner is mounted on a 2-D traversing table while the optical system remains fixed.

Velocity measurements are made in the radial direction at three axial locations for swirl number ( $S$ ) of 1.0, fuel-swirl air momentum flux ratio ( $MR$ ) of 1.5, and axial fuel injection. The radial profiles of normalized turbulent kinetic energy and mean axial and radial velocities at three axial locations ( $X/D = 0.6, 2.0,$  and  $4.0$ ) are shown in Fig. 3. The centerline axial velocity is positive at all downstream locations indicating the penetration of fuel jet through the recirculation zone. The first point of zero crossing of the axial velocity ( $R = 4$  mm) and the outer radial position of the peak velocity ( $R = 14$  mm) indicate the width of the recirculation zone. The location of the maximum radial velocity also indicates the lateral boundary of the recirculation zone. The normalized maximum turbulent kinetic energy distributes near the edge of the recirculation zone indicating strong turbulent mixing at this location.

Multi-point Raman/LIPF-OH measurements along the radial direction of the swirling methane jet flame are performed at three downstream locations ( $X/D = 0.6, 2.0,$  and  $4.0$ ). The single-pulse species concentrations and temperatures are averaged over 200 laser shots. Radial profiles of temperature and mole fraction for three downstream locations are shown in Fig. 4. The profiles show that temperature increases with increasing radial and axial positions. The maximum mean flame temperature appears at the mixing layer between the recirculation zone and the ambient air ( $R = 14$  mm) where the combustion products of  $H_2O$  and  $CO_2$  and the maximum turbulent kinetic energy occurs. There is essentially no reaction in the center of the jet for all the measured downstream locations, because  $CH_4$  is not consumed and no products are formed. The slightly higher temperature (400-600 K) is due to heating from the combustion occurred at the mixing layer between the fuel jet and the recirculation zone. The Raman measurements confirm the velocity measurements that the fuel jet penetrates through the recirculation zone. The width of the plateau in the  $O_2$ ,  $H_2O$ , and  $CO_2$  profiles indicates the width of the recirculation zone. The width of the recirculation zone determined from the Raman measurements is also consistent with that measured from the velocity profiles. The  $CO$  concentration is formed in the recirculation zone near the jet exit ( $X/D = 0.6$ ). Further downstream ( $X/D = 2.0$  and  $4.0$ )  $CO$  is burned at the radial position beyond the recirculation boundary. It should be noted that methane is decomposed and  $H_2$  is formed at the shear layer near the nozzle exit ( $X/D = 0.6$ ). More  $H_2$  is formed and diffused into the fuel jet and the recirculation zone as it moves further downstream. The  $OH$  profiles indicate that combustion takes place in three regions; the mixing layer between the fuel jet and the recirculation zone ( $R = 2.5$  mm), inside the recirculation zone ( $R = 4 - 13$  mm), and the thin layer between the recirculation zone and the ambient air ( $R = 14$  mm). The peak value of  $OH$  (0.025) at  $R = 2.5$  mm is much higher than that in the recirculation zone and that at  $R = 14$  mm for  $X/D = 0.6, 2.0,$  and  $4.0$ . However, the temperature distributes in an inverse way. This is due to the superequilibrium  $OH$  that surpasses the equilibrium value at local temperature.

### Acknowledgment

This research was supported by the National Science Council of the Republic of China under the grant numbers NSC87-2212-E-216-007 (TSC), NSC87-2212-E-006-080 (YCC), and NSC87-2212-E-006-081 (TY). The financial supports are gratefully acknowledged.

### References

- Brockhinke, A., Andresen, P., and Kohse-Höinghaus, K., (1995) *Appl. Phys. B* **61**, pp. 533-545.
- Chen, R. H. and Driscoll, J. F., (1988) *Twenty-Second Symposium (International) on Combustion*, The Combustion Institute, Pittsburgh, PA, pp. 531-540.
- Chen, R. H. and Driscoll, J. F., (1990) *Twenty-Third Symposium (International) on Combustion*, The Combustion Institute, Pittsburgh, PA, pp. 281-288.
- Chen, Y.-C., Peters, N., Schneemann, G. A., Wruck, N., Renz, U., and Mansour, M. S., (1996) *Combust. Flame*, **107**, pp. 223-244.
- Cheng, T. S., Wehrmeyer, J. A., and Pitz, R. W., (1992). *Combust. Flame*, **91**, pp. 323-345.
- Cheng, T. S., Wehrmeyer, J. A., Pitz, R. W., Jarrett, O., and Northam, G. B., (1994) *Combust. Flame*, **99**, pp. 157-173.
- Cheng, T. S., Yuan, T., Chao, Y.-C., Lu, C.-C., and Wu, D.-C., (1998a) *Combust. Sci. and Tech.*, Vol. 135, pp. 65-84.

- Cheng, T. S., Chao, Y.-C., Wu, D.-C., Yuan, T., and Lu, C.-C., (1998b) *Twenty-Seventh Symposium (International) on Combustion*, The Combustion Institute, Pittsburgh, PA.
- Chigier, N. A., Beér, J. M., Grecov, D., and Bassindale, K., (1970) *Combust. Flame* 14: 171-180.
- Claypole, T. C., and Syred, N., (1981) *Eighteenth Symposium (International) on Combustion*, The Combustion Institute, Pittsburgh, PA, pp. 81-89.
- Drake, M. C., Pitz, R. W., and Lapp, M. (1986) *AIAA J.* 24, pp. 905-917.
- Eckbreth, A. C., (1988). *Laser diagnostics for combustion temperature and species*. Abacus, Cambridge, Mass.
- Hassel, E. P., (1993) *Applied Optics*, 32, pp. 4058-4065.
- Mansour, M. S. and Chen, Y. C. (1996) *Applied Optics*, 35, pp. 4252-4260.
- Nandula, S. P., Brown, T. M., and Pitz, R. W., (1994) *Combust. Flame*, 99, pp. 775-783.

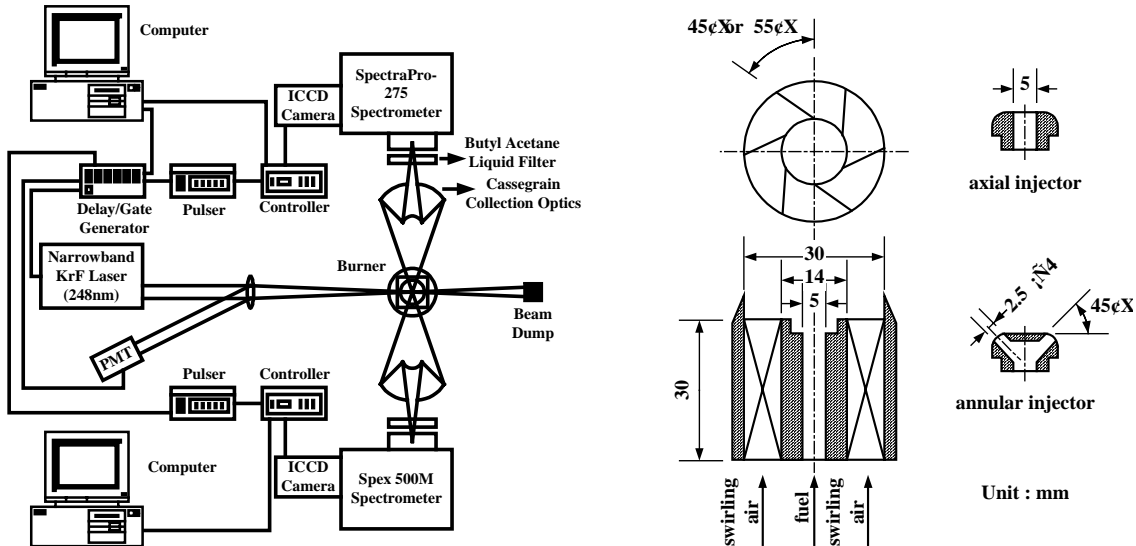


Fig. 1 Schematic diagram of the Raman/LIPF-OH system. Fig. 2 Schematic diagram of the swirling burner.

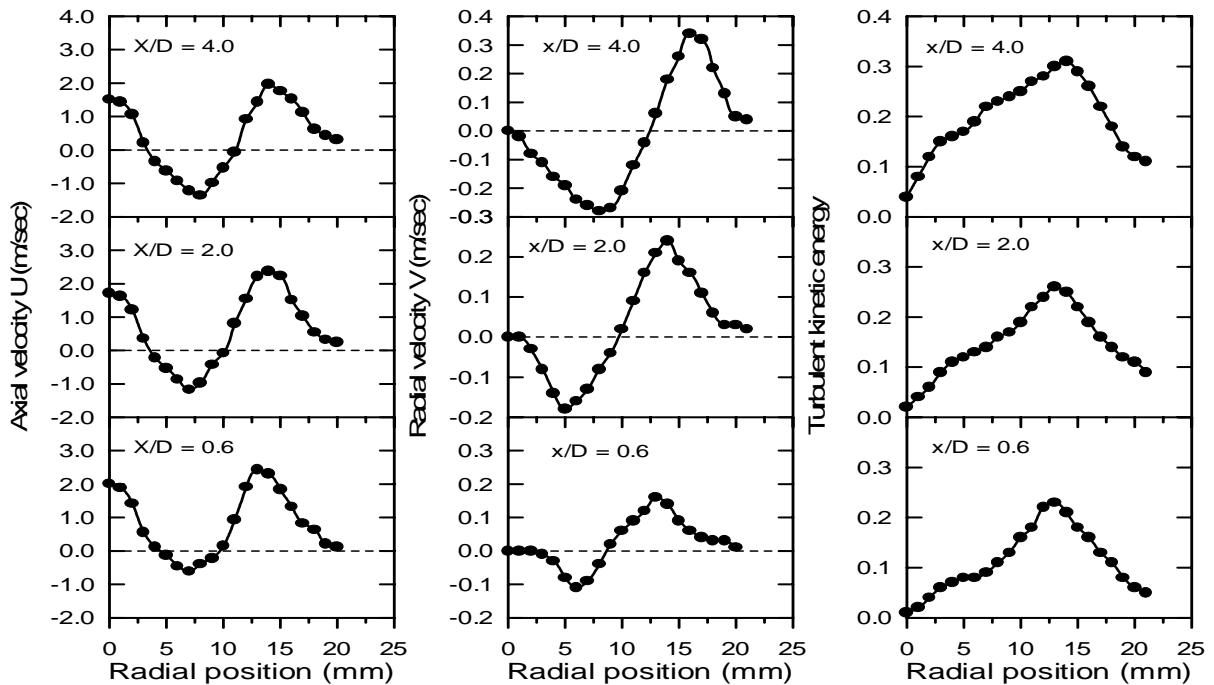


Fig. 3 Radial profiles of mean axial and radial velocities and normalized turbulent kinetic energy ( $k / U_A$ ) for the fuel jet-dominated flame ( $S = 1.0$ ,  $MR = 1.50$ ) with axial fuel injection. Turbulent kinetic energy  $k = (u'^2 + v'^2 + w'^2)/2$ .  $U_A$  is the calculated swirling air exit velocity.

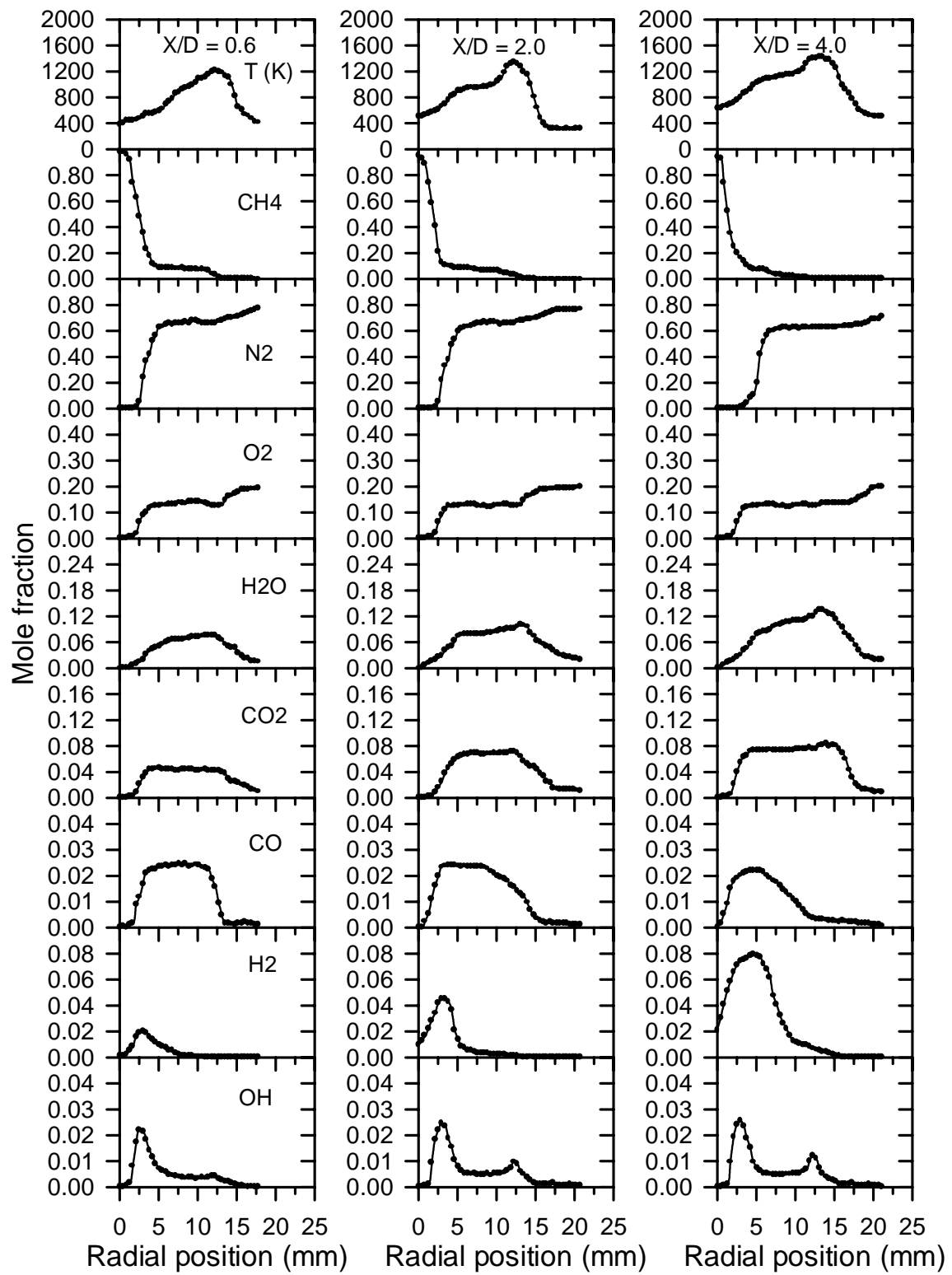


Fig. 4 Averaged (200 shots) radial profiles of temperature and species concentrations in the swirling methane jet flame ( $S = 1.0$ ,  $MR = 1.5$ ) with axial fuel injection at  $X/D = 0.6$ ,  $2.0$ , and  $4.0$ .